Adsorption of an Alternating Copolymer near a Fluid–Fluid Interface

Weixiong Li,[†] Chuck Yeung,[†,‡] David Jasnow,[‡] and Anna C. Balazs*[,†]

Materials Science and Engineering Department, University of Pittsburgh, Pittsburgh, Pennsylvania 15261, and Department of Physics and Astronomy, University of Pittsburgh, Pittsburgh, Pennsylvania 15260

Received January 22, 1992; Revised Manuscript Received April 17, 1992

ABSTRACT: We use numerical methods and analytical analysis to determine the behavior of a single alternating AB copolymer at a liquid–liquid interface. Monomers of type A favor fluid 1, while B monomers prefer fluid 2. Using the transfer matrix formalism, we calculate the monomer density profile near the interface and determine the phase diagram. This phase diagram contains two delocalized phases and a localized phase. We determine the scaling behavior for the localization length as a function of the monomer–solvent interaction energies. An effective potential is derived that correctly explains the scaling behavior observed in our numerical studies.

Introduction

Amphiphilic copolymers are highly effective at stabilizing oil–water emulsions and microemulsions. Due to the presence of both hydrophobic and hydrophilic segments, the chains may be adsorbed at the oil–water interface, where they can reduce the interfacial tension by as much as 2 orders of magnitude.[1] As a consequence, these polymeric emulsifiers form critical components in the fabrication of products that range from cosmetics to herbicides.[1] In order to design the optimal emulsifers, it becomes necessary to establish how the molecular architecture of the chains affects these interfacial properties. In this paper, we examine the behavior of an alternating AB copolymer at the boundary between two immiscible liquids. We demonstrate that the conformation of the chain at the interface is dramatically sensitive to the arrangement of the monomers (the sequence distribution) in the copolymer. Specifically, the scaling behavior that characterizes this chain conformation displays a unique exponent for the strictly alternating architecture: its value is different from that obtained for other copolymer sequence distributions.[2]

In addition to probing the role of molecular architecture, we examine the effect of varying the relative affinities between the monomers and the two different fluids. Through this study, we can determine conditions under which the alternating chain becomes "delocalized", i.e., drifts away from the interface and is preferentially located in one of the two liquids.

Below, we describe the model we used to analyze these issues. We then compare our findings with the results obtained for other copolymer architectures at a penetrable interface[2-4] and discuss the consequences of our findings on the interfacial behavior of amphiphilic copolymers.

The Model

The interface between the two immiscible fluids is represented by the $z = 0$ plane. Thus, the boundary is taken to be sharp and stationary. We consider a single Gaussian chain, whose length approaches infinity. This polymer is composed of an equal number of A and B monomers ($N_A = N_B$), which are arranged in a strictly alternating pattern along the polymer (...ABABAB...). The monomers interact with the fluid through the following potentials:

$$U_A(z) = -\Delta_A \operatorname{sgn}(z)$$

$$U_B(z) = +\Delta_B \operatorname{sgn}(z) \tag{1}$$

where Δ_A and Δ_B represent the respective monomer–solvent interaction energies. For $\Delta_A, \Delta_B \geq 0$, the A monomers prefer the $z > 0$ region, while B monomers favor the $z < 0$ domain. We first consider the behavior of the polymer chain for the symmetric case where $\Delta_A = \Delta_B \equiv \Delta$. We will then discuss the asymmetric case ($\Delta_A \neq \Delta_B$) and present a phase diagram in the ($\Delta_A - \Delta_B$) space.

The Green's function of a Gaussian copolymer subject to the potential given by eq 1 is[5]

$$G(\{z_i\}) \propto \prod_{n=\text{even}} \exp\left\{-\frac{3}{2}[(z_{n-1}-z_n)^2 + (z_n - z_{n+1})^2] - \Delta_B \operatorname{sgn}(z_n)\right\} \exp\left\{\frac{1}{2}\Delta_A[\operatorname{sgn}(z_{n-1}) + \operatorname{sgn}(z_{n+1})]\right\} \tag{2}$$

Here, we have assigned even indices to B monomers and odd indices to A monomers. The x and y components of the Green's function have been integrated out and are not included in eq 2. Equation 2 is invariant under the transformations

$$\Delta_A \leftrightarrow \Delta_B \quad \text{and} \quad z \rightarrow -z \tag{3}$$

and

$$\Delta_A \rightarrow -\Delta_A, \quad \Delta_B \rightarrow -\Delta_B, \quad z \rightarrow -z \tag{4}$$

Therefore, we only have to consider the region $\Delta_A \geq \Delta_B \geq 0$.

The partition function is the integral of the Green's function over all the coordinates z_k. We can focus on the A monomers by integrating out all the degrees of freedom associated with the B's. After discarding all the constant factors, we get the partition function

$$\Psi = \int \prod_{n=\text{even}} K(z_{n-1}, z_{n+1})\, dz_{n-1} \tag{5}$$

where

$$K(x,y) = I\left(\frac{x+y}{2}, \Delta_B\right) \exp\left\{-\frac{3}{4}(x-y)^2 + \frac{1}{2}\Delta_A[\operatorname{sgn}(x) + \operatorname{sgn}(y)]\right\} \tag{6}$$

[†] Materials Science and Engineering Department.
[‡] Department of Physics and Astronomy.

0024-9297/92/2225-3685$03.00/0

and

$$I(t,\Delta) = \exp(\Delta)\ \mathrm{erfc}\ (3^{1/2}t) + \exp(-\Delta)\ \mathrm{erfc}\ (-3^{1/2}t) \quad (7)$$

The A monomer density is defined as

$$\rho_A(z) = \left\langle \frac{1}{N_A} \sum_{k=\mathrm{odd}} \delta(z_k - z) \right\rangle \quad (8)$$

where we have normalized $\rho_A(z)$ by the total number of A monomers in the chain. The brackets $\langle\ \rangle$ indicate an average over all possible configurations; in other words

$$\rho_A(z) = \frac{1}{\Psi} \int \frac{1}{N_A} \sum_{k=\mathrm{odd}} \delta(z_k - z) \prod_{n=\mathrm{even}} K(z_{n-1}, z_{n+1})\, \mathrm{d}z_{n-1} \quad (9)$$

We solve eqs 5 and 9 by using a transfer matrix approach under periodic boundary conditions. The associated eigenvalue equation of the kernel K is

$$\int_{-\infty}^{\infty} K(x,y)\ \phi(y)\ \mathrm{d}y = \lambda\phi(x) \quad (10)$$

(Since the kernel $K(x,y)$ is symmetric, both λ and ϕ are real.) In the infinite chain limit, the monomer density $\rho_A(z)$ becomes

$$\rho_A(z) = [\phi_0(z)]^2 \quad (11)$$

where $\phi_0(z)$ is the eigenvector corresponding to the largest eigenvalue, normalized so that

$$\int_{-\infty}^{\infty} [\phi_0(z)]^2\, \mathrm{d}z = 1 \quad (12)$$

Finally, we define the width of the density profile (the localization width) as

$$w = \left[\int_{-\infty}^{\infty} z^2 \phi_0^{\,2}(z)\, \mathrm{d}z\right]^{1/2} \quad (13)$$

Delocalization is signaled by the divergence of w.

Numerical Results

We numerically solve eq 10 for $\phi_0(z)$ using an iterative method. In numerical computations, this integral must be cut off at finite values $|z| < R$. For a well-localized state, the width of the density profile w is much smaller than R. Consequently, the solution does not depend on the value of R. If the state is delocalized or has a localization width $w \gg R$, the final solution is strongly dependent on the value of R. When the latter behavior is observed, we subsequently choose a relatively large value of R and vary the values of Δ_A and Δ_B along various contours (say $\Delta_A - \Delta_B$ is equal to various constants) in the phase space $\Delta_A - \Delta_B$. The locations at which the width w becomes comparable to R are regarded as estimates of localization–delocalization transition points. This approximate criterion is sufficiently accurate since w is extremely sensitive to Δ_A and Δ_B near the transition point. (See the following discussion of Figure 3.)

Figure 1 shows the monomer density $\rho_A(z)$ for the symmetric case $\Delta_A = \Delta_B \equiv \Delta$, at $\Delta = 0.141, 0.2, 0.3, 0.4$, and 0.5. The integration is cut off at $R = 160$, which is much larger than the widths of the profiles. Consequently, for these values of Δ, the chain is localized at the interface. The density profiles show a discontinuous jump at the interface $z = 0$, which is due to the jump in the potential that each monomer experiences. As the value of Δ becomes smaller, the density profile gets wider, indicating that the adsorption is weaker and the chain is swollen. At the same time, the discontinuous jump in the density profiles becomes smaller. This is due to the smaller difference in interaction energy of the monomers in the two liquids.

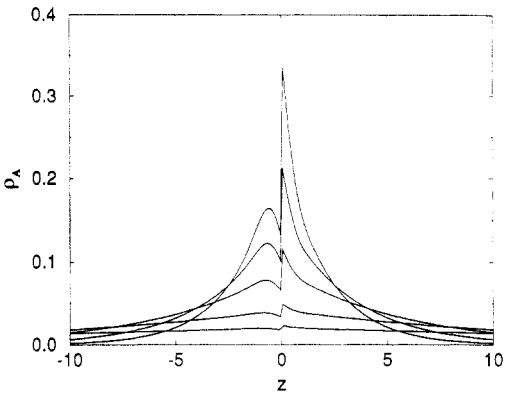

Figure 1. Density profiles of A monomers $\rho_A(z)$ at $\Delta_A = \Delta_B = \Delta = 0.141, 0.2, 0.3, 0.4$, and 0.5. The density profiles become wider as Δ gets smaller.

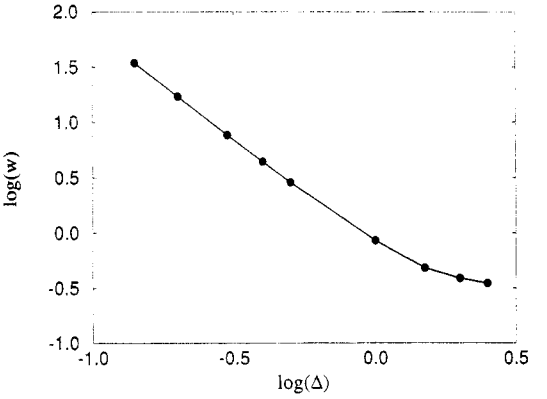

Figure 2. log–log plot of the localization lengths versus Δ. In the small Δ region, the behavior is linear with a slope of −2.

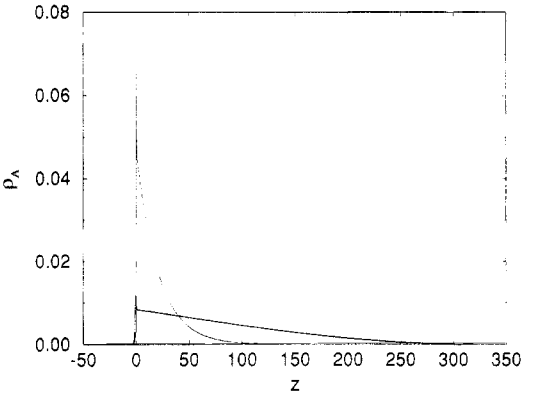

Figure 3. Density profiles at two points $(\Delta_A, \Delta_B) = (0.7, 0.6)$ (the narrower curve) and (0.69, 0.59) (the wider curve) along the line $\Delta_A - \Delta_B = 0.1$, respectively. As one approaches the transition point, the density profiles spread out rapidly.

The widths of the density profiles are plotted in Figure 2 as a function of Δ on a log–log scale. In the region where Δ is small and the width w is large (the "weak adsorption" region), the localization width behaves as $w \sim \Delta^{-2}$. On the other hand, as Δ increases, w approaches a limiting value.

When Δ_A and Δ_B are unequal, localization–delocalization transitions occur for finite differences between Δ_A and Δ_B. To illustrate the transition, we calculate the density profiles along the straight line $\Delta_A - \Delta_B = 0.1$. Figure 3 shows the densities $\rho_A(z)$ at two points $(\Delta_A, \Delta_B) = (0.7, 0.6)$ (the narrower curver) and (0.69, 0.59) (the wider curve) along this line, respectively. Note that for these curves, the integration cutoff is at $R = 320$. Thus, for the curve with $\Delta_A = 0.7$ and $\Delta_B = 0.6$, the solution is accurate since $w = 27.9 \ll 320$. On the other hand, the profile with Δ_A

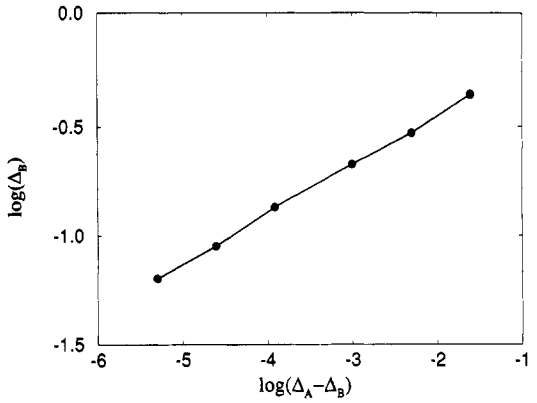

Figure 4. log (Δ_B) versus log ($\Delta_A - \Delta_B$) along the phase boundary separating the localized and the delocalized phases. Near the region $\Delta_A = \Delta_B = 0$ the exponent is roughly 4.

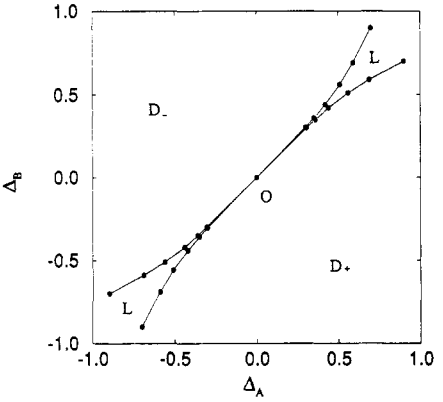

Figure 5. Proposed phase diagram in the $\Delta_A - \Delta_B$ parameter space. D_+ and D_- are phases where the polymer is delocalized in $z > 0$ and $z < 0$ regions, respectively. L is the localized phase. The four phase boundaries transform into one another under the transformations in eqs 3 and 4.

= 0.69 and $\Delta_B = 0.59$ is more spread out, and the solution shows a strong dependence on the cutoff value R. The localization length must be greater than the cutoff R. Thus $(\Delta_A, \Delta_B) = (0.69, 0.59)$ represents a rough estimate of the transition point. In this way, other transition points are also estimated and plotted in Figure 4. In the weak adsorption limit (small Δ), we find that the localization–delocalization transition line $\Delta_A - \Delta_B = f(\Delta_B)$ approaches the origin $\Delta_A = \Delta_B = 0$ with an exponent approximately equal to 4; i.e., $\Delta_A - \Delta_B \simeq \Delta_B^4$.

Figure 5 shows our proposed phase diagram, including negative values of Δ_A and Δ_B. L represents the localized phase for which the width w is finite. D_+ and D_- are the two delocalized phases in which the polymer chain is delocalized in the $z > 0$ and $z < 0$ regions, respectively. The four transition lines meet at the origin tangentially, with an apparent common slope of 1.

An interesting question is whether the density profiles (Figure 3) widen continuously or discontinuously. Unfortunately, numerical studies cannot answer this question conclusively. In our discussion of the effective potential analysis (below), we shall point out that such a transition is likely to be continuous.

Analytical Results and Discussion

The above numerical results can be understood by a careful analysis of the kernel $K(x,y)$ in eq 6. For small Δ_B, the function $I(x,\Delta_B)$ can be written as

$$I(x,\Delta_B) = 1 + \Delta_B S(x) + \frac{1}{2}\Delta_B^2 + \ldots$$

$$\simeq \exp\left\{\Delta_B S(x) + \frac{1}{2}\Delta_B^2[1 - S(x)^2]\right\} + O(\Delta_B^3) \quad (14)$$

where

$$S(x) = \frac{1}{2}[\mathrm{erfc}\,(3^{1/2}x) - \mathrm{erfc}\,(-3^{1/2}x)] \quad (15)$$

and we have only kept terms up to Δ_B^2. We now make an essential approximation by writing

$$I\left(\frac{x+y}{2},\Delta_B\right) \simeq \frac{I(x,\Delta_B) + I(y,\Delta_B)}{2} \quad (16)$$

This approximation requires small values of Δ_B and is valid when the chain is not significantly stretched, thereby assuring that neighboring monomers are close to one another. Substituting eqs 14 and 16 into the kernal $K(x,y)$ in eq 6, we find the chain becomes a Gaussian homopolymer of effective monomer size $2^{1/2}$ in an effective potential

$$U_{\mathrm{eff}}(z) = -\Delta_A\,\mathrm{sgn}\,(z) - \Delta_B S(z) - \frac{1}{2}\Delta_B^2[1 - S(z)^2] \quad (17)$$

Let us first consider the symmetric case $\Delta_A = \Delta_B \equiv \Delta$. In this case, the effective potential vanishes rapidly at large distances. In the infinite chain limit, the monomer density is the square of the ground state wave function of the following equation:

$$-\frac{1}{3}\frac{d^2\psi(z)}{dz^2} + U_{\mathrm{eff}}(z)\,\psi(z) = E\psi(z) \quad (18)$$

At large distances, $U_{\mathrm{eff}}(z)$ can be neglected, and the wave function decays exponentially as $\exp[-(-3E)^{1/2}z]$. That is, the localization width $w \sim 1/(-3E)^{1/2}$. For small Δ, we can use a result from quantum mechanics:[6] In one dimension, for a weak potential that vanishes sufficiently rapidly at large z

$$(-E)^{1/2} \propto \int_{-\infty}^{\infty} U_{\mathrm{eff}}(z)\,dz \quad (19)$$

The terms linear in Δ in U_{eff} (eq 17) do not contribute to the integral eq 19 since sgn (z) and $S(z)$ are odd functions of z. Therefore, the decay length is proportional to $1/(-E)^{1/2} \propto \Delta^{-2}$, agreeing with the numerical results in Figure 2. This novel scaling behavior is due to the cancellation of the monomer interactions when the monomers are at large distances from the interface.

When $\Delta_A > \Delta_B$, the effective potential no longer vanishes at large distances; instead, it has values $\pm(\Delta_A - \Delta_B)$ as $z \to \mp\infty$, respectively. We rewrite the effective potential in eq 17 as the sum of two terms: one term depends only on Δ_B and the second term depends only on $\Delta_A - \Delta_B$

$$U_{\mathrm{eff}}(z) = U^0_{\mathrm{eff}}(z) - (\Delta_A - \Delta_B)\,\mathrm{sgn}\,(z) \quad (20)$$

where $U^{(0)}_{\mathrm{eff}}(z)$ is obtained by replacing Δ_A by Δ_B in the first term in eq 17. The second term in eq 20 distorts the original wave function associated with $U^{(0)}_{\mathrm{eff}}$. For small Δ_B, the energy level of this wave function is on the order of $-\Delta_B^4$ according to eq 19. Therefore, when $\Delta_A - \Delta_B$ is on the order of this ground-state energy level, the original ground state will be sufficiently distorted and may be delocalized; this heuristic argument is consistent with the empirical behavior $\Delta_A - \Delta_B \sim \Delta_B^4$ marking the phase boundary in Figure 4.

We now consider the nature of the localization–delocalization transition. Zia et al.[7] discussed the existence and nature of bound states in one-dimensional quantum mechanical systems having potentials with a variety of analytic forms. Our effective potential in eq 17 is extremely short ranged: it decays rapidly with a Gaussian tail. Straightforward extensions of the results of Zia et al. for short-range potentials show that the localization–delo-

calization transition will be continuous. That is, the inverse of the localization width, w^{-1}, goes to zero continuously at the transition. This is similar to the situation in critical wetting in two dimensions, which can also be analyzed by mapping the problem into one-dimensional quantum mechanics.[8] Finally we comment that the origin ($\Delta_A = \Delta_B = 0$) in Figure 5 is special: four critical lines meet there with common slopes. This may be reminiscent of a tetracritical point in critical phenomena. Such an analogy, however, is not perfect since, at the origin in the phase diagram, there is no chain–interface interaction. As we cross the origin from D_+ into D_-, we find that the polymer chain shifts from the $z > 0$ region to the $z < 0$ region discontinuously.

We can compare our results with previous studies. Garel et al.[3] studied a model in which the monomers interact with the fluids through the potential

$$U(z) = u \operatorname{sgn}(z) \tag{21}$$

where u for each monomer is an independent Gaussian random variable. They found that a transition between a localized state and a delocalized state occurs as one varies the center of the Gaussian distribution. In particular, when the Gaussian distribution is centered around 0, the polymer is always localized. Yeung et al.[2] observed that for a symmetric AB copolymer, whose sequence distribution ranges from blocky to nearly alternating, the width of the polymer layer is always finite. Furthermore, the width scales as Δ^{-1} in the weak adsorption limit. Marques and Joanny[4] studied various models of polymer adsorption. In particular, they examined the case where $N_A \gg N_B$ and the A monomers are distributed periodically along the length of the chain. In the weak adsorption limit, they showed that the width of the polymer interface scales as the inverse of the interaction strength, agreeing with a scaling argument of de Gennes.[9]

Our results are in qualitative agreement with those of Garel et al.[3] in the following sense. In the symmetric case, $\Delta_A = \Delta_B \equiv \Delta$, the polymer is always localized at finite Δ. Localization–delocalization transitions take place at finite values of Δ_A and Δ_B when $\Delta_A \neq \Delta_B$. When Δ_A is sufficiently larger than Δ_B, A monomers strongly prefer to stay in the $z > 0$ region so that they drag B monomers along with them, delocalizing the polymer in the region $z > 0$. This finding, along with the results of Garel et al.,[3] shows that sufficient asymmetry in monomer–fluid interaction will delocalize the polymer from the interface. In the weak adsorption limit, in contrast to the results in refs 2–4, the localization length in our model diverges as Δ^{-2}. This different scaling relation shows the sensitivity of adsorption properties on polymer structures.

Finally, we discuss the case where the chain consists of an alternating sequence of p monomers instead of one monomer; i.e., the chain is $...A_pB_pA_pB_p...$. We now argue that, in the case where $\Delta_A = \Delta_B \equiv \Delta$ is small, there exists an optimal and finite value of p so that the chain is most localized at the interface. For small values of p, increasing p will increase the effective interactions between these blocks and the solvent, an effect that tends to bind the chain more tightly to the interface. On the other hand, when p is sufficiently large, A's will stay predominantly in the $z > 0$ region, while the B's will remain in the $z < 0$ region. In this case the localization length behaves as $p^{1/2}$, which is an increasing function of p. We thus conclude that an optimal p exists that minimizes the localization length.

Conclusions

In summary, we have examined the adsorption properties of an alternating chain near a fluid–fluid interface. We numerically calculated the monomer density profiles and from them determined the phase diagram. Our main results are as follows: First, along the symmetric ($\Delta_A = \Delta_B \equiv \Delta$) line, the localization length w diverges as Δ^{-2} in the weak adsorption limit. We also derive an effective potential that successfully explains this scaling relation. Second, for the asymmetric case ($\Delta_A > \Delta_B$), we find that localization–delocalization transitions occur at finite values of $\Delta_A - \Delta_B$. For small Δ_A and Δ_B, this transition occurs when $\Delta_A - \Delta_B \sim \Delta_B^4$. Our effective potential also reveals scaling behavior that is consistent with our empirical findings. From the monomer density profiles, we present the complete phase diagram.

Acknowledgment. We thank T. Burkhardt for useful conversations. A.C.B. gratefully acknowledges financial support from the Office of Naval Research, through Grant N00014-91-J-1363, the National Science Foundation, through Grant DMR-9107102, and PPG Industries. D.J. gratefully acknowledges support from the National Science Foundation, through Grant DMR89-14621, and the Pittsburgh Supercomputer Center.

References and Notes

(1) Hancock, R. I. *Surfactants*; Tadros, Th. F., Ed.; Academic Press: New York, 1984; p 287.
(2) Yeung, C.; Balazs, A. B.; Jasnow, D. *Macromolecules* **1992**, *25*, 1357.
(3) Garel, T.; Huse, D. A.; Leibler, S.; Orland, H. *Europhys. Lett.* **1989**, *8*, 13.
(4) Marques, C. M.; Joanny, J. F. *Macromolecules* **1990**, *23*, 268.
(5) For a discussion of Gaussian chains, see: Doi, M.; Edwards, S. F. *The Theory of Polymer Dynamics*; Clarendon Press: Oxford, U.K., 1986.
(6) Landau, L. D.; Lifshitz, E. M. *Quantum Mechanics: Non-relativistic Theory*; Pergamon Press: Oxford, U.K., 1958; pp 155 and 156, problem 1.
(7) Zia, R. K. P.; Lipowsky, R.; Kroll, D. M. *Am. J. Phys.* **1988**, *56*, 160.
(8) See ref 7 and references therein.
(9) de Gennes, P.-G. *Scaling Concepts in Polymer Physics*; Cornell University Press: Ithaca, NY, 1979.